JACS
JOURNAL OF THE AMERICAN CHEMICAL SOCIETY

Communication

pubs.acs.org/JACS

Electric Field-Induced Assembly of Monodisperse Polyhedral Metal–Organic Framework Crystals

Nobuhiro Yanai,[†,‡,§,⊥] Melinda Sindoro,[‡,§] Jing Yan,[†] and Steve Granick*[,†,‡,∥]

[†]Department of Materials Science and Engineering, [‡]Department of Chemistry, and [∥]Department of Physics, University of Illinois, Urbana, Illinois 61801, United States

Supporting Information

ABSTRACT: Monodisperse polyhedral metal–organic framework (MOF) particles up to 5 μm in size, large enough to enable *in situ* optical imaging of particle orientation, were synthesized by the strategy of simultaneous addition of two capping ligands with different binding strength during crystallization. Upon dispersing them in ethylene glycol and applying AC electric field, the particles facets link to form linear chains. We observe well-regulated crystal orientation not only for rhombic dodecahedra all of whose facets are equivalent, but also for truncated cubes with nondegenerate facets. After removing the electric field, chains disassemble if their facets contain even modest curvature, but remain intact if their facets are planar. This assembly strategy offers a general route to fabricate oriented polyhedral crystal arrays of potential interest for new applications and functions.

The polyhedral morphology of crystalline particles opens, in principle, a pathway to enlarge the scope of colloidal self-assembly with structures unobtainable with conventional spherical particles.[1−3] This, in turn, might enlarge functionality beyond what is possible with conventional nonspherical particles made from amorphous polymer or oxides such as silica.[4−9] Here, we investigate the approach of on-demand activation of well-controlled attachments between the crystal facets of particles whose size is colloidal. To accomplish this, we apply AC electric field to induce dipolar attractions between particles suspended in fluid, which can be a general strategy.[10] This proven technique for the manipulating of spherical colloids[11,12] has not to our knowledge been applied previously to assembling faceted crystals. Here, first we describe methods to synthesize polyhedral crystals of the needed dimensions. Then, we describe what determines the perfection of oriented strings of such crystals.

This study is based on a new extension of nanoporous materials referred to as metal–organic frameworks (MOFs) or porous coordination polymers (PCPs).[13−21] Traditionally, MOFs are viewed from the perspective of bulk materials with random orientation, but recently, it has become evident that the capacity to engineer crystal arrangements should open the door to advanced applications.[3,22−29] For example, the control of crystal orientation would align the pores and maximize the separation capacities.[30] Aligned MOF channels are also useful to orient functional guest molecules anisotropically.[31,32] Periodic supracrystal architectures are useful for photonic and sensing applications.[33,34] For these purposes, assembling preformed MOF crystals offers potential to be a general method because it utilizes simple physical interactions to direct the particles without need for specific chemically induced attraction.[3,28,29] The scheme in Figure 1 shows that facet-to-facet attachments would lead to well-defined orientational order of polyhedral crystals. Here, our choice of assembly induced by external field is motivated by our desire to obviate the need for selective surface functionalization.

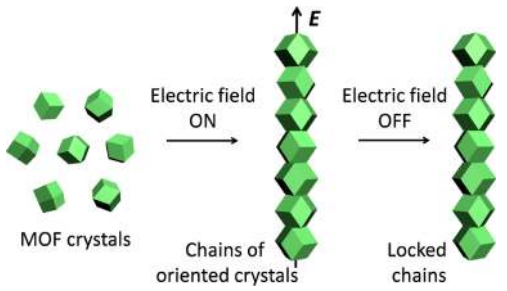

Figure 1. Scheme according to which electric field assembles MOF crystals into chains with orientational order, the particles remaining locked into stable chains when electric field is switched off.

While prior literature teaches one how to produce monodisperse MOF crystals of nanoscale dimension,[35,36] this study required development of monodisperse polyhedra with dimensions measured in micrometers, in order to allow *in situ* optical imaging of the mutual orientation of distinct crystal facets.[3] This problem was solved synthetically by introducing dual capping ligands in the MOF synthesis such that two capping reagents with different binding strength worked in a concerted manner. We applied this strategy to the prototypical MOF, $[Zn(mim)_2]_n$ (ZIF-8; mim = 2-methylimidazolate). The idea is as follows. It was known that introduction of a capping ligand such as 1-methylimidazole (1-MI) into the ZIF-8 synthesis suppresses nucleation points, which increases the final crystal size of ZIF-8.[36] However, the size of such crystals is too small (~1 μm) to visualize the facets even by high-resolution microscopy.[3] We also were unsuccessful in growing larger crystals merely by modulating 1-MI concentration since the crystal size decreases with increase of the 1-MI concentration above 100 mM, probably because 1-MI suppresses not only nucleation but also crystal growth (Table

Received: September 21, 2012

 © XXXX American Chemical Society dx.doi.org/10.1021/ja309361d | J. Am. Chem. Soc. XXXX, XXX, XXX–XXX

S1). One possible route to further increase the crystal size was introduction of a relatively weaker ligand, poly(vinyl pyrrolidone) (PVP; M_w = 360 000) in this work, which helped to further decrease the number of nucleation points without suppressing crystal growth. We found that when PVP was exclusively used as a capping ligand, the crystal size increased from 64 to 140 nm. Thus, PVP acts as a relatively weak ligand, as these increments are much less than the case for 1-MI (size up to ~800 nm).

Remarkably, the concurrent employment of both 1-MI and PVP resulted in crystal size as large as 5.3 μm (Figure 2a, Table S1). The observed increase of particle size with increasing concentration of 1-MI and PVP suggests that 1-MI and PVP suppressed nucleation cooperatively. Scanning electron microscopy (SEM) characterization showed that the particles were close to uniform in size with distinct rhombic dodecahedron morphology and flat facets (Figure S1). Polydisperse particles were formed at very high concentration of 1-MI (200 mM) probably because of secondary nucleation. No precipitation was obtained above 250 mM of 1-MI due to the complete suppression of crystal nucleation and growth.

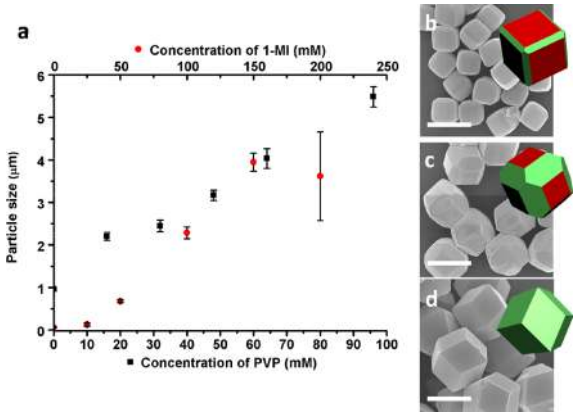

Figure 2. Crystal size and morphology controlled by two capping ligands. (a) Crystal size of ZIF-8 synthesized in the presence of various concentrations of capping ligands, 1-MI and PVP. Black dots show dependence of particle size on PVP concentration (1-MI is fixed at 100 mM), while red dots show dependence on 1-MI concentration (PVP is fixed at 32 mM). Concentrations of $Zn(NO_3)_2{\cdot}6H_2O$ and Hmim were fixed at 25 and 100 mM, respectively. SEM images of ZIF-8 crystals crystallized for (b) 1, (c) 3, and (d) 20 h (3.7 μm in size). Scale bars = 3 μm. Schematic representations of the three crystal morphologies are shown as insets.

Particle shape changes dramatically as these crystals grow.[36] Initially, slightly truncated cubes form with dominant square {100} facets and small hexagonal {110} facets (Figure 2b). As these cubes grew, the relative area of {110} facets increases and the crystal morphology evolves first to truncated rhombic dodecahedra, then finally to rhombic dodecahedra (Figure 2c,d).

We found that PVP stabilizes the intermediate morphologies exhibiting {100} facets. Crystals synthesized without added PVP are unstable in MeOH and their facets etch away after prolonged incubation (Figure S2), but the presence of PVP during incubation prevents etching by stabilizing the crystal facets with surface-adsorbed PVP chains, a phenomenon that we deduced from observed decrease of the zeta potential. Rhombic dodecahedra synthesized without PVP typically have a zeta potential of +48 mV, but this decreased to +20 mV after PVP functionalization, presumably owing to charge screening by adsorbed PVP.[37] When PVP was introduced during the crystal synthesis, the obtained rhombic dodecahedra displayed a lower zeta potential of +12 mV, reflecting more charge screening by higher PVP density on crystal facets. Note that the zeta potential observed for rhombic dodecahedra is similar to that measured for truncated cubes (+14 mV) and truncated rhombic dodecahedra (+10 mV). As expected, these intermediate morphologies synthesized with PVP were stable in the fluid-dispersed form. This enabled us to investigate their assembly.

For visualization using confocal microscopy, the ZIF-8 surfaces were functionalized with a fluorescent dye containing an imidazole group (BODIPY), following a method previously described by this laboratory.[3] The dye-modified rhombic dodecahedra shown in Figure 2d were dispersed in ethylene glycol and sandwiched to thickness 50 μm between two indium tin oxide (ITO) coated coverslips. An AC electric field (1 MHz, 200 V/mm) was applied perpendicular to the ITO surfaces. Data were acquired at 40 planar images/s. Under the electric field, cross-sectional shapes of discrete particles showed no preferred crystal orientations (Figure S3).

We describe now directed assembly under electric field. Particles attached to one another within seconds after coming into proximity; this was slow enough to image by confocal microscopy, but sufficiently rapid to be effective. Strikingly, the polyhedra reoriented to form facet-to-facet contacts; visually, this was clear by observing that the cross-sectional outlines of crystals changed to elongated hexagons, which indicates the ⟨110⟩ orientation of crystals parallel to the direction of electric field (Figure S3). Within a few minutes, stepwise successive growth by this process formed 1-D chains oriented in the direction of the electric field (Figure 3a, Movie S1).

The observed elongated hexagonal cross sections at the centers of the polyhedra and their rhombic facets at the particle−particle contacts confirm crystal orientation throughout the chains (Figures 3b and S4). The fact that the centers of hexagonal cross sections of different crystals were located close

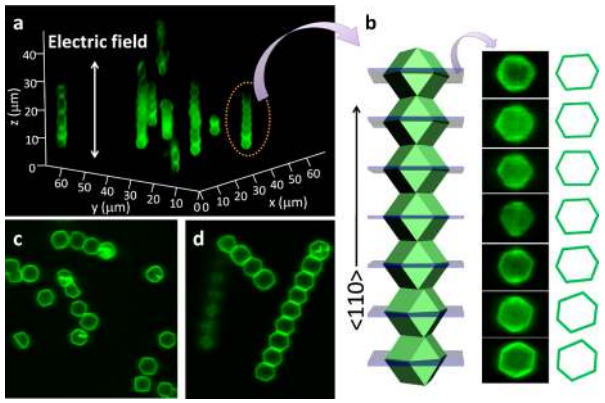

Figure 3. Electric field assembly of rhombic dodecahedra. (a) Typical *in situ* observation of 1-D chains of rhombic dodecahedra (Figure 2d) along the direction of electric field (1 MHz, 200 V/mm) by confocal microscopy. (b) Confocal cross sections perpendicular to the electric field, along with schematic representations of contour. Elongated hexagonal outlines indicate the ⟨110⟩ orientation of crystals along the direction of electric field. (c) Disconnected chains of rhombic dodecahedra after turning off the AC field (1 MHz, 200 V/mm). (d) Stably locked chains of rhombic dodecahedra after turning off the AC field (1 kHz, 200 V/mm).

dx.doi.org/10.1021/ja309361d | J. Am. Chem. Soc. XXXX, XXX, XXX−XXX

to each other along the chain indicates considerable overlap at the contact between {110} crystal facets, resulting in ⟨110⟩ orientation of crystals along the chain. This configuration minimizes the center-to-center separation between particles, probably serving to maximize the dipole−dipole interaction.[10] However, in directions perpendicular to the electric field, the orientation differed between cross-sectional hexagons, probably owing to thermal fluctuations. After the electric field was switched off, the chains fell apart (Figure 3c, S5).

Two AC frequencies were employed, 1 kHz and 1 MHz. We observed chain formation at both frequencies (Figure S6), but interestingly, chains constructed at 1 kHz remained stable after turning off the electric field (Figure 3d), the chains simply sedimenting to the bottom ITO surface. It is known that at low frequency the dominant mechanism of attraction is the polarization of electrostatic double layer rather than the dielectric polarization of particle itself which dominates at high frequency (1 MHz).[38,39] The former mechanism would favor direct surface-to-surface contact for particles with flat facets, allowing polyhedra to overcome electrostatic repulsion and come sufficiently close together that van der Waals attraction causes them to adhere. To exclude the alternative explanation that adhesion reflected surface bridging by PVP chains, we performed a control experiment using particles coated with silica (zeta potential = −46 mV); these silica-coated particles similarly formed stable chains under the same conditions of electric field. Thus, it appears that van der Waals attractions held adjoining facets together.

Exploring further this assembly under electric field, we examined MOF crystals with other morphologies. The truncated rhombic dodecahedra (Figure 2c) also formed 1-D chains along the direction of electric field (1 kHz; Figure S7). The crystal orientation of this complex morphology was then examined with chains lying on the bottom ITO surface after turning off the field (Figure 4a). The cross-sectional views at different heights showed that crystals of ⟨110⟩ and ⟨100⟩ orientation coexist within the same chain. It seems that, in this case, the electric field could not differentiate between the {110} and {100} facets, perhaps because their area difference was too small.

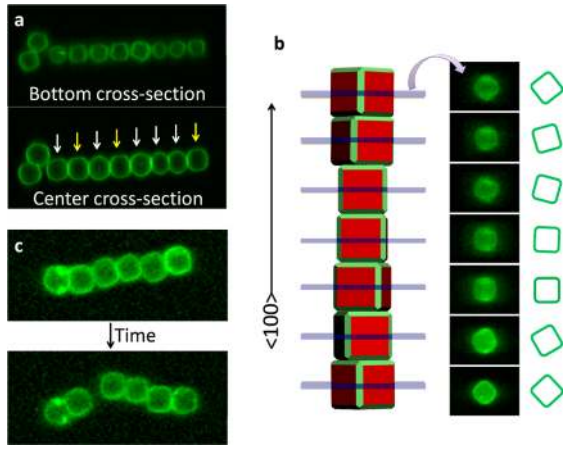

Figure 4. (a) Typical chains of truncated rhombic dodecahedra (Figure 2c) after turning off the electric field (1 kHz, 200 V/mm) and allowing chains to sediment. White and yellow arrows represent crystals with ⟨110⟩ and ⟨100⟩ orientations along the chain direction, respectively. (b) Cross sections of truncated cubes (Figure 2b) in a 1-D chain under electric field (1 kHz, 200 V/mm). The square outlines with rounded corners indicate the ⟨100⟩ orientation of crystals along the direction of electric field. (c) Spontaneous breakage of a chain of truncated cubes after removing the electric field (1 kHz, 200 V/mm).

Meanwhile, facet-selective attachment was observed for truncated cubes (Figure 2b), for which the {100} facets are much larger than the {110} facets. Forests of chains were observed to form (1 kHz; Figure S8, Movie S2). The observed square cross sections with rounded corners demonstrate that the larger {100} facets selectively attach to each other, resulting in ⟨100⟩ orientation of crystals along the direction of electric field (Figure 4b). However, in contrast to the stable chains of rhombic dodecahedra, the locking between truncated cubes was not permanent; after turning off the field, the chains fell apart with time due to Brownian motion (Figure 4c, Movie S3).

We carried out atomic force microscopy (AFM) measurements of these crystals (Figure S9). The observed {110} facets of rhombic dodecahedra are quite flat—not concave, not convex. On the other hand, the truncated cubes possess convex {100} facets, with the center being 60 nm higher than the edge. The van der Waals attraction between these convex {100} facets must then be much less than that between flat {110} facets of rhombic dodecahedra purely due to geometric reason. This explains the difference in chain stability for these two morphologies. Although it is possible in principle to stabilize chains of simple spheres by welding them together with polymer layers,[40] this study shows that simple van der Waals attraction can also accomplish this, provided that the facets are sufficiently flat. Considerations of zeta potential cannot explain the differences, as zeta potential is similar for both these polyhedra.

To sum up, this study articulates design rules to direct chain formation of polyhedral crystals by means of electric field. First, dipolar attractions between crystals appear to drive preferential facet-to-facet attachment. Second, selective attachment between facets appears to be possible by manipulating surface area and surface curvature. Third, facet flatness encourages the formation of chains locked into place even after external field is removed.

Looking to the future, we remark that chain length can be lengthened if desired, as the technical path to do so by further design of the electrodes is known.[40] Presently it is typically around 10 particles, but sometimes spans the entire distance between the electrodes. With higher particle concentration, it would also be possible to form 3-D structures with intriguing packing geometry between them. Paths are also clear to spatially pattern the supracrystal architectures by using lithographically patterned electrodes.[41] Although it is not yet possible using the simple, prototypical MOF particles employed in this work, whose pore networks are isotropic, rational generalization of these approaches using anisotropic 1-D channel systems, may allow anisotropic molecular flow along chain structures of the kind produced here.

■ ASSOCIATED CONTENT

Ⓢ Supporting Information

Experimental detail, particle synthesis summary, SEM, confocal microscopy, AFM results. This material is available free of charge via the Internet at http://pubs.acs.org.

■ AUTHOR INFORMATION

Corresponding Author

sgranick@illinois.edu

dx.doi.org/10.1021/ja309361d | J. Am. Chem. Soc. XXXX, XXX, XXX−XXX

Present Address

[⊥]Department of Chemistry and Biochemistry, Graduate School of Engineering, and Center for Molecular Systems (CMS), Kyushu University, Fukuoka 819-0395, Japan.

Author Contributions

[§]These authors contributed equally.

Notes

The authors declare no competing financial interest.

■ ACKNOWLEDGMENTS

This work was supported at the University of Illinois by the US Army Research Office (grant award no. W911NF-10-1-0518). NY. acknowledges a JSPS postdoctoral fellowship for research abroad.

■ REFERENCES

(1) Henzie, J.; Grunwald, M.; Widmer-Cooper, A.; Geissler, P. L.; Yang, P. D. *Nat. Mater.* **2012**, *11*, 131−137.
(2) Young, K. L.; Jones, M. R.; Zhang, J.; Macfarlane, R. J.; Esquivel-Sirvent, R.; Nap, R. J.; Wu, J. S.; Schatz, G. C.; Lee, B.; Mirkin, C. A. *Proc. Natl. Acad. Sci. U.S.A.* **2012**, *109*, 2240−2245.
(3) Yanai, N.; Granick, S. *Angew. Chem., Int. Ed.* **2012**, *51*, 5638−5641.
(4) Glotzer, S. C.; Solomon, M. J. *Nat. Mater.* **2007**, *6*, 557−562.
(5) Jiang, S.; Chen, Q.; Tripathy, M.; Luijten, E.; Schweizer, K. S.; Granick, S. *Adv. Mater.* **2010**, *22*, 1060−1071.
(6) Rossi, L.; Sacanna, S.; Irvine, W. T. M.; Chaikin, P. M.; Pine, D. J.; Philipse, A. P. *Soft Matter* **2011**, *7*, 4139−4142.
(7) Sacanna, S.; Pine, D. J. *Curr. Opin. Colloid Interface Sci.* **2011**, *16*, 96−105.
(8) Zhao, K.; Bruinsma, R.; Mason, T. G. *Proc. Natl. Acad. Sci. U.S.A.* **2011**, *108*, 2684−2687.
(9) Rice, R.; Roth, R.; Royall, C. P. *Soft Matter* **2012**, *8*, 1163−1167.
(10) Jones, T. B. in *Electromechanics of Particles*; Chembridge University Press: New York, NY, 1995.
(11) Leunissen, M. E.; Christova, C. G.; Hynninen, A.-P.; Royall, C. P.; Campbell, A. I.; Imhof, A.; Dijkstra, M.; van Roij, R.; van Blaaderen, A. *Nature* **2005**, *437*, 235−240.
(12) Sullivan, M. T.; Zhao, K.; Hollingsworth, A. D.; Austin, R. H.; Russel, W. B.; Chaikin, P. M. *Phys. Rev. Let.* **2006**, *96*, 015703.
(13) Yaghi, O. M.; O'Keeffe, M.; Ockwig, N. W.; Chae, H. K.; Eddaoudi, M.; Kim, J. *Nature* **2003**, *423*, 705−714.
(14) Kitagawa, S.; Kitaura, R.; Noro, S.-i. *Angew. Chem., Int. Ed.* **2004**, *43*, 2334−2375.
(15) Férey, G.; Serre, C. *Chem. Soc. Rev.* **2009**, *38*, 1380−1399.
(16) Lee, J.; Farha, O. K.; Roberts, J.; Scheidt, K. A.; Nguyen, S. T.; Hupp, J. T. *Chem. Soc. Rev.* **2009**, *38*, 1450−1459.
(17) Li, J. R.; Kuppler, R. J.; Zhou, H.-C. *Chem. Soc. Rev.* **2009**, *38*, 1477−1504.
(18) Inokuma, Y.; Kawano, M.; Fujita, M. *Nat. Chem.* **2011**, *3*, 349−358.
(19) Horcajada, P.; Gref, R.; Baati, T.; Allan, P. K.; Maurin, G.; Couvreur, P.; Férey, G.; Morris, R. E.; Serre, C. *Chem. Rev.* **2012**, *112*, 1232−1268.
(20) Wu, H. H.; Gong, Q. H.; Olson, D. H.; Li, J. *Chem. Rev.* **2012**, *112*, 836−868.
(21) Sumida, K.; Rogow, D. L.; Mason, J. A.; McDonald, T. M.; Bloch, E. D.; Herm, Z. R.; Bae, T. H.; Long, J. R. *Chem. Rev.* **2012**, *112*, 724−781.
(22) Biemmi, E.; Scherb, C.; Bein, T. *J. Am. Chem. Soc.* **2007**, *129*, 8054−8055.
(23) Shekhah, O.; Wang, H.; Kowarik, S.; Schreiber, F.; Paulus, M.; Tolan, M.; Sternemann, C.; Evers, F.; Zacher, D.; Fischer, R. A.; Wöll, C. *J. Am. Chem. Soc.* **2007**, *129*, 15118−15119.
(24) Zacher, D.; Shekhah, O.; Wöll, C.; Fischer, R. A. *Chem. Soc. Rev.* **2009**, *38*, 1418−1429.
(25) Ameloot, R.; Gobechiya, E.; Uji-i, H.; Martens, J. A.; Hofkens, J.; Alaerts, L.; Sels, B. F.; De Vos, D. E. *Adv. Mater.* **2010**, *22*, 2685−2688.
(26) Carbonell, C.; Imaz, I.; Maspoch, D. *J. Am. Chem. Soc.* **2011**, *133*, 2144−2147.
(27) Umemura, A.; Diring, S.; Furukawa, S.; Uehara, H.; Tsuruoka, T.; Kitagawa, S. *J. Am. Chem. Soc.* **2011**, *133*, 15506−15513.
(28) Tsotsalas, M.; Umemura, A.; Kim, F.; Sakata, Y.; Reboul, J.; Kitagawa, S.; Furukawa, S. *J. Mater. Chem.* **2012**, *22*, 10159−10165.
(29) Pang, M.; Cairns, A. J.; Liu, Y.; Belmabkhout, Y.; Zeng, H. C.; Eddaoudi, M. *J. Am. Chem. Soc.* **2012**, *134*, 13176.
(30) Bloch, E. D.; Queen, W. L.; Krishna, R.; Zadrozny, J. M.; Brown, C. M.; Long, J. R. *Science* **2012**, *335*, 1606−1610.
(31) Cui, H. B.; Wang, Z. M.; Takahashi, K.; Okano, Y.; Kobayashi, H.; Kobayashi, A. *J. Am. Chem. Soc.* **2006**, *128*, 15074−15075.
(32) Koh, K.; Wong-Foy, A. G.; Matzger, A. J. *J. Am. Chem. Soc.* **2010**, *132*, 15005−15010.
(33) Kreno, J. E.; Leorg, K.; Farha, O. K.; Allendorf, M.; Van Duyne, R. P.; Hupp, J. T. *Chem. Rev.* **2012**, *112*, 1105−1125.
(34) Wu, Y.; Li, F.; Zhu, W.; Cui, J.; Tao, C.; Lin, C.; Hannam, P. M.; Li, G. *Angew. Chem., Int. Ed.* **2011**, *50*, 12518−12522.
(35) Tsuruoka, T.; Furukawa, S.; Takashima, Y.; Yoshida, K.; Isoda, S.; Kitagawa, S. *Angew. Chem., Int. Ed.* **2009**, *48*, 4739−4743.
(36) Cravillon, J.; Nayuk, R.; Springer, S.; Feldhoff, A.; Huber, K.; Wiebcke, M. *Chem. Mater.* **2011**, *23*, 2130−2141.
(37) Goncharuk, E. V.; Pakhovchishin, S. V.; Zarko, V. I.; Gun'ko, V. M. *Colloid J.* **2001**, *63*, 283−289.
(38) Basuray, S.; Chang, H.-C. *Phys. Rev. E* **2007**, *75*, 060501.
(39) Wei, M. T.; Junio, J.; Ou-Yang, H. D. *Biomicrofluidics* **2009**, *3*, 012003.
(40) Vutukuri, H. R.; Demirçrs, A. F.; Peng, B.; van Oostrum, P. D. J.; Imhof, A.; van Blaaderen, A. *Angew. Chem., Int. Ed.* **2012**, *51*, 11249−11253.
(41) Hayward, R. C.; Saville, D. A.; Aksay, I. A. *Nature* **2000**, *404*, 56−59.